

DO-TH 97/22
DTP/97/90
October 1997

Radiative Parton Model Analysis of Recent Polarized DIS Data

Marco Stratmann*

Institut für Physik, Universität Dortmund, 44221 Dortmund, Germany

and

Department of Physics, University of Durham, Durham DH1 3LE, England[†]

Abstract

An updated next-to-leading order (NLO) QCD analysis of the spin asymmetries $A_1^N(x, Q^2)$ and parton distributions $\delta f(x, Q^2)$ in longitudinally polarized deep-inelastic lepton-nucleon scattering is presented within the framework of the radiative parton model taking into account recent experimental results. The theoretical framework and the main features of the radiative parton model analysis are briefly reviewed. The small- x behaviour of the polarized structure function $g_1^N(x, Q^2)$ as well as the shape of the polarized gluon distribution $\delta g(x, Q^2)$ are shown to be still hardly constrained by present fixed target data.

*Invited talk presented at the workshop 'Deep Inelastic Scattering off Polarized Targets: Theory Meets Experiment', DESY-Zeuthen, Germany, September 1-5, 1997

[†]Present address

Radiative Parton Model Analysis of Recent Polarized DIS Data

Marco Stratmann

Institut für Physik, Universität Dortmund, 44221 Dortmund, Germany

and

Department of Physics, University of Durham, Durham DH1 3LE, England[†]

Abstract

An updated next-to-leading order (NLO) QCD analysis of the spin asymmetries $A_1^N(x, Q^2)$ and parton distributions $\delta f(x, Q^2)$ in longitudinally polarized deep-inelastic lepton-nucleon scattering is presented within the framework of the radiative parton model taking into account recent experimental results. The theoretical framework and the main features of the radiative parton model analysis are briefly reviewed. The small- x behaviour of the polarized structure function $g_1^N(x, Q^2)$ as well as the shape of the polarized gluon distribution $\delta g(x, Q^2)$ are shown to be still hardly constrained by present fixed target data.

1 Introduction

The past year has seen much progress in our knowledge about the nucleons' spin structure due to new experimental results on the spin asymmetry $A_1^N(x, Q^2) \simeq g_1^N(x, Q^2)/F_1^N(x, Q^2)$ in deep-inelastic scattering with longitudinally polarized lepton beams off nucleon targets ($N = p, n, d$). In particular, previous sparse and not very precise experimental information on the neutron asymmetry A_1^n [1] has been succeeded by more accurate data by the E154 collaboration [2] where also the kinematical coverage in x and Q^2 was slightly extended. Recently the HERMES group also has presented first results on A_1^n [3] and preliminary data for a proton target (A_1^p) have been reported on this workshop [4]. SMC has released a new detailed analysis of A_1^p [5] which does not indicate a rise of g_1^p at small- x anymore and, finally, first very accurate, but still preliminary results from E155 on g_1^p were also presented on this workshop [6].

In view of these recent experimental developments it seems to be worthwhile to reanalyse [7] these data¹ in terms of polarized parton distributions δf in the framework of perturbative QCD. Preceding studies [8, 9, 10] have revealed that the detailed x -shape of the polarized gluon distribution $\delta g(x, Q^2)$ was only weakly constrained by the data of that time even though a tendency towards a sizeable positive *total* gluon polarization, $\int_0^1 \delta g(x, Q^2 = 4 \text{ GeV}^2) dx \gtrsim 1$, was found [8, 9, 10]. It is thus interesting to study to what extent these old results are confirmed by the new data sets and whether one can further pin down the polarized gluon distribution.

[†]Present address

¹The preliminary E155 [6] and HERMES [4] proton data are not available yet and hence not included in our analysis so far.

In the following we will concentrate exclusively on calculations of A_1^N to NLO accuracy which became possible only recently after the derivation of the required spin-dependent two-loop anomalous dimensions [11, 12]. A first such complete and consistent NLO study has been presented in [8] (based on a corresponding LO analysis [13]), where the underlying concept has been the radiative generation of parton distributions from a valence-like structure at some low bound-state like resolution scale μ . In the unpolarized case this had previously led [14, 15], e.g., to the successful prediction of the small- x rise of the proton structure function F_2^p as later on observed at HERA. Other NLO analyses of polarized DIS data can be found in [9, 10].

In the next section the basic theoretical framework for polarized DIS beyond the leading order is briefly discussed hereby defining our notations, and the main features of the radiative parton model analysis [8] are reviewed. Section 3 contains the presentation and discussion of the new quantitative NLO QCD results and, finally, the main findings are summarized in section 4.

2 Theoretical Framework

Measurements of polarized deep inelastic lepton nucleon scattering yield direct information [1-6,16] only on the spin-asymmetry

$$A_1^N(x, Q^2) \simeq \frac{g_1^N(x, Q^2)}{F_1^N(x, Q^2)} = \frac{g_1^N(x, Q^2)}{F_2^N(x, Q^2)/[2x(1 + R^N(x, Q^2))]} \quad , \quad (1)$$

where $N = p, n, d$ (in the latter case we have used $g_1^d = \frac{1}{2}(g_1^p + g_1^n)(1 - \frac{3}{2}\omega_D)$ with $\omega_D = 0.058$) and $R \equiv F_L/2xF_1 = (F_2 - 2xF_1)/2xF_1$. In NLO, the polarized structure function $g_1^N(x, Q^2)$ in (1) is related to the spin-dependent quark and gluon distributions (δf^N) in the following way:

$$g_1^N(x, Q^2) = \frac{1}{2} \sum_q e_q^2 \left\{ \delta q^N(x, Q^2) + \delta \bar{q}^N(x, Q^2) + \frac{\alpha_s(Q^2)}{2\pi} [\delta C_q \otimes (\delta q^N + \delta \bar{q}^N) + \delta C_g \otimes \delta g] \right\} \quad (2)$$

with the convolutions (\otimes) being defined as usual. The NLO pieces entering (2), i.e., δf^N , δC_q , δC_g , depend on the factorization convention (scheme) adopted. Since the two-loop anomalous dimensions of [11, 12] refer to the conventional $\overline{\text{MS}}$ dimensional regularization prescription we prefer to work also in this scheme. The appropriate spin-dependent $\overline{\text{MS}}$ Wilson coefficients δC_q and δC_g can be found, e.g., in [11, 8]. It should be recalled that the first moment $\Gamma_1^N(Q^2) \equiv \int_0^1 g_1^N(x, Q^2) dx$ of eq. (2) is in the $\overline{\text{MS}}$ scheme simply given by

$$\Gamma_1^N(Q^2) = \frac{1}{2} \sum_q e_q^2 \left(1 - \frac{\alpha_s(Q^2)}{\pi} \right) [\Delta q^N(Q^2) + \Delta \bar{q}^N(Q^2)] \quad (3)$$

where we have introduced the first moments $\Delta f^N(Q^2)$ of the polarized distributions $\delta f^N(x, Q^2)$ by defining as usual

$$\Delta f^N(Q^2) \equiv \int_0^1 \delta f^N(x, Q^2) dx \quad (4)$$

where $f = u, \bar{u}, d, \bar{d}, s, \bar{s}$, and g and have used (see, e.g., [11, 8]) $\int_0^1 \delta C_q(x) dx = -3C_F/2$ and $\int_0^1 \delta C_g(x) dx = 0$. Thus, the total gluon helicity $\Delta g(Q^2)$ does not directly couple to $\Gamma_1^N(Q^2)$ due to the vanishing of the integrated gluonic coefficient function in the $\overline{\text{MS}}$ factorization scheme. Other factorization schemes [10] are of course also allowed but afford a proper scheme transformation

(which cannot be uniquely fixed) such that the physical quantity g_1^N remains scheme independent up to $\mathcal{O}(\alpha_s)$.

The NLO Q^2 -evolution of the polarized parton distributions $\delta f(x, Q^2)$ (henceforth we shall, as always, use the notation $\delta q^p \equiv \delta q$ and $q^p \equiv q$) governed by the two-loop anomalous dimensions [11, 12] is performed most conveniently in the Mellin- n moment space where the solutions of the evolution equations (see, e.g., refs.[14, 8]) can be obtained analytically, once the boundary conditions at some $Q^2 = Q_0^2$, i.e., input densities $\delta f(x, Q_0^2)$ to be discussed below, are specified. Furthermore, in Mellin- n space the convolutions in (2) reduce to simple products. Having obtained the analytic NLO solutions for the moments of parton densities or the analogous n -space expression of (2) the desired x -space results for $\delta f(x, Q^2)$ or $g_1^N(x, Q^2)$ are then simply obtained by a standard numerical Mellin inversion as described, e.g., in [14].

In our analysis only quarks with $m_q < \Lambda_{QCD}$, i.e., u, d, s , will be treated as light partons in the evolution equations while the charm contribution to g_1^N (as well as to F_1^N) is calculated via the appropriate massive $\gamma^* g \rightarrow c\bar{c}$ fusion process [17] although it turns out (see later) that in the kinematical region covered by present fixed target experiments [1-6,16] the charm contribution is extremely small and practically irrelevant.

To finally fix the NLO input parton densities $\delta f(x, Q_0^2)$ we perform fits only to the *directly measured* spin asymmetry $A_1^N(x, Q^2)$ in (1), rather than to the derived $g_1^N(x, Q^2)$. The main reason for that is that in some older experimental analyses $g_1^N(x, Q^2)$ has been extracted under the assumption of the Q^2 -independence of $A_1^N(x, Q^2)$, which is - although presently available data do not exhibit any significant Q^2 -dependence within the experimental errors - theoretically not warranted due to the different Q^2 -evolutions of the numerator and denominator in (1).

As already mentioned in the introduction, the other main ingredient of our NLO analysis [8] is that we follow the radiative (dynamical) concept [14, 15] by choosing the same low input scale $Q_0^2 = \mu^2 = 0.34 \text{ GeV}^2$ and implementing the fundamental positivity requirement

$$|\delta f(x, Q^2)| \leq f(x, Q^2) \quad (5)$$

down to $Q^2 = \mu^2$. The analysis affords some well established set of unpolarized NLO parton distributions $f(x, Q^2)$ for calculating $F_1^N(x, Q^2)$ in (1) and as reference distributions in (5) which will be adopted from ref.[15].

In addition to (5), the first moments $\Delta f(Q^2)$ of the NLO polarized parton distributions are taken to be subject to two very different sets of theoretical constraints [13, 8] related to two different views concerning the flavor $SU(3)_f$ symmetry properties of hyperon β -decays. One set ('standard' scenario) assumes an unbroken $SU(3)_f$ symmetry between the relevant matrix elements leading to the following sum rule constraints,

$$\Delta q_3 = \Delta u + \Delta \bar{u} - \Delta d - \Delta \bar{d} = g_A = F + D = 1.2573 \pm 0.0028 \quad (6)$$

$$\Delta q_8 = \Delta u + \Delta \bar{u} + \Delta d + \Delta \bar{d} - 2(\Delta s + \Delta \bar{s}) = 3F - D = 0.579 \pm 0.025 \quad (7)$$

with the values of g_A and $3F - D$ taken from [18]. It should be noted that the flavor non-singlet combinations $\Delta q_{3,8}$ in (6) and (7) remain Q^2 -independent also in NLO [11, 12, 8].

As a plausible alternative to the full $SU(3)_f$ symmetry between charged weak and neutral axial currents required for deriving the 'standard' constraints (6) and (7), we consider a 'valence' scenario [13, 19] where this flavor symmetry is broken and which is based on the assumption [19] that the flavor changing hyperon β -decay data fix only the total helicity of *valence* quarks:

$$\Delta u_V(\mu^2) - \Delta d_V(\mu^2) = g_A = F + D = 1.2573 \pm 0.0028 \quad (8)$$

$$\Delta u_V(\mu^2) + \Delta d_V(\mu^2) = 3F - D = 0.579 \pm 0.025 \quad (9)$$

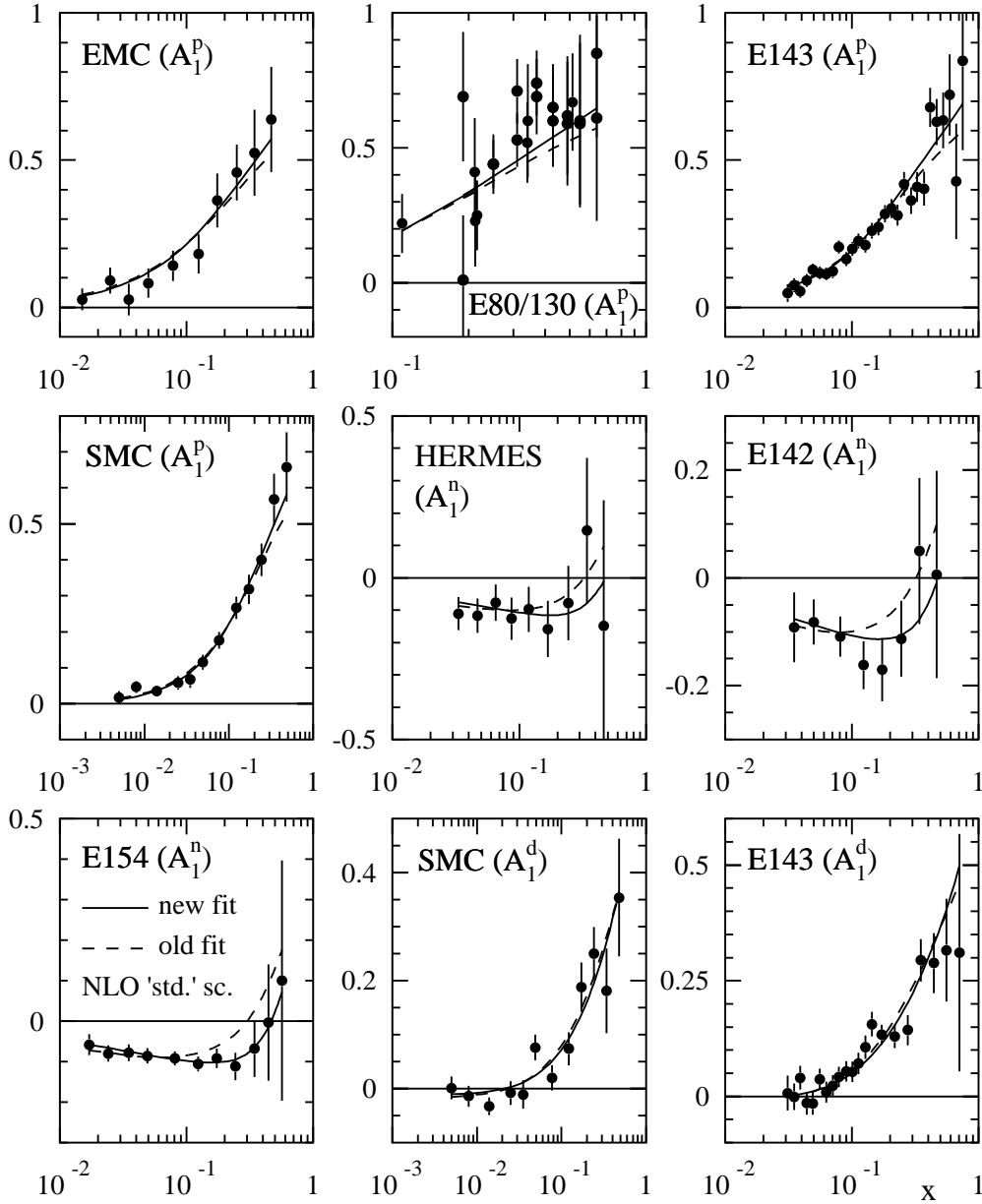


Figure 1: Comparison of our reanalysed NLO 'standard' results for $A_1^N(x, Q^2)$ (solid lines) with all presently available data [1-3,5,16]. The Q^2 values adopted here correspond to the different values quoted in [1-3,5,16]. Also shown are the results of our previous analysis [8] (dashed lines).

The 'standard' scenario always requires a finite total strange sea helicity of $\Delta s = \Delta \bar{s} \simeq -0.05$ in order to account for the experimentally observed reduction of Γ_1^p with respect to the Gourdin and Ellis and Jaffe estimate [20]. Within the 'valence' scenario, on the contrary, a negative light sea helicity $\Delta \bar{u} = \Delta \bar{d} \equiv \Delta \bar{q} \simeq -0.07$ alone suffices and we shall assume a maximally $SU(3)_f$ broken polarized strange sea input $\delta s(x, \mu^2) = \delta \bar{s}(x, \mu^2) = 0$ here [8]. Finally, we note that in both above scenarios the Bjorken sum rule manifestly holds due to the constraints (6), (8).

3 Quantitative NLO Results

Turning to the determination of the polarized NLO parton distributions $\delta f(x, Q^2)$ it is helpful to consider some reasonable and simple, but still sufficiently flexible ansatz for the $\delta f(x, \mu^2)$ with

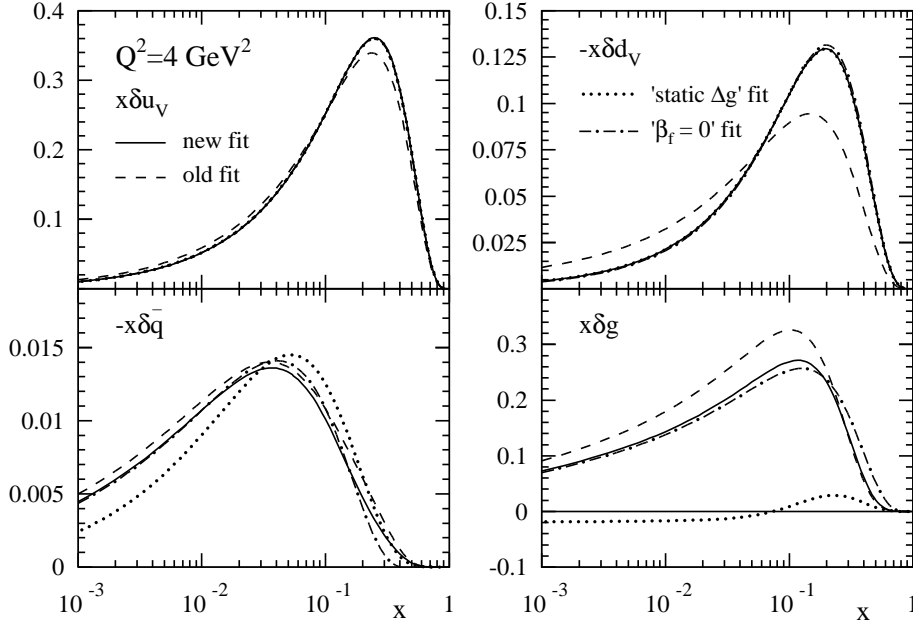


Figure 2: The polarized NLO $\overline{\text{MS}}$ densities at $Q^2 = 4 \text{ GeV}^2$ in the 'standard' scenario as obtained in our new and old [8] analyses. Also shown are the distributions obtained in two other fits employing some extra constraints on the input distributions. It should be noted that as a result of the fits the sea always turns out to be $SU(3)_f$ symmetric, i.e., $\bar{q} \equiv \bar{u} = \bar{d} = \bar{s}$.

not too many free parameters. As a general ansatz we take [8]

$$\delta f(x, \mu^2) = N_f x^{\alpha_f} (1-x)^{\beta_f} f(x, \mu^2) \quad (10)$$

where $f = u_V, d_V, \bar{q} \equiv \bar{u} = \bar{d}, s, g$ which links the polarized input distributions to the unpolarized ones as taken from [15] (in this way the positivity requirements (5) can be trivially implemented). One can argue that the available inclusive DIS data do not allow for a fully flavor-decomposed ansatz like (10) but instead only for a separation into non-singlet, singlet and gluon distributions. This is of course true, but the aim of our analysis is not only to simply fit the available data but also to provide a realistic set of parton distributions which can be further probed in processes other than DIS, i.e., to have 'predictive power'. For obvious reasons, we have not taken into account any $SU(2)_f$ breaking input ($\delta\bar{u} \neq \delta\bar{d}$) in (10). Moreover the number of parameters in (10) can be further reduced without any worsening of the fit by setting $\beta_{u_V} = \beta_{d_V} = 0$, $\alpha_s = 0$, and $\beta_s = 0$ in (10).

A comparison of our best fit employing the 'standard' scenario constraints (6) and (7) with the available data on $A_1^N(x, Q^2)$ [1-3,5,16] is presented in fig. 1. Also shown are the results for A_1^N obtained by using our previous fit results [8]. The results in the 'valence' scenario are indistinguishable from the ones shown and hence suppressed. The total χ^2 of the 'new' and 'old' optimal 'standard' scenario fits is 123.02 and 144.37, respectively, for 168 data points. As can be inferred from fig. 1 the results for the proton (A_1^p) as well as for the deuteron (A_1^d) are basically not affected by the reanalysis despite of the rather large differences in the neutron case (A_1^n) mainly due to the rather precise, new E154 data [2]. This can be understood better by comparing the individual parton distributions $\delta f(x, Q^2)$ rather than A_1^N itself. This is done in fig. 2 for the 'new' and 'old' [8] NLO $\overline{\text{MS}}$ densities at $Q^2 = 4 \text{ GeV}^2$. As can be seen from fig. 2 apart from a slightly smaller gluon distribution δg only δd_V changes by quite a large amount.

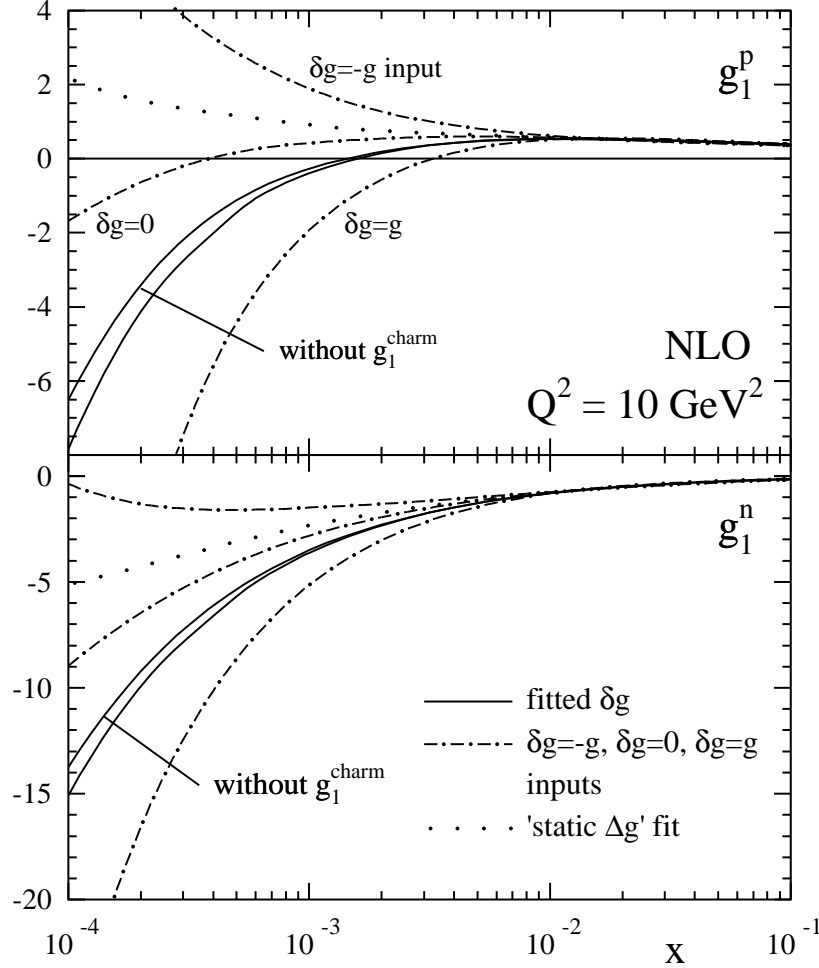


Figure 3: The small- x behaviour of g_1^p (upper part) and g_1^n (lower part) in NLO at $Q^2 = 10 \text{ GeV}^2$ as predicted by various 'standard' scenario fits employing different boundary conditions for the polarized input gluon distribution $\delta g(x, \mu^2)$. For the optimal fit input also the effect of not including the charm contribution to $g_1^{p,n}$ is shown.

This is because δd_V is mainly probed in g_1^n (i.e., A_1^n) where we have observed the largest changes as compared to our old results [8] in fig. 1.

Also shown in fig. 2 are the results of two other fits which are based on some additional constraints on the input distributions. For the ' $\beta_f = 0$ ' fit we have set $\beta_f = 0$ in our ansatz (10). The total χ^2 of 123.6 is very similar to our best fit and this confirms the results of a recent fit by the E154 collaboration [21] based on our radiative parton model framework [8] where all β 's were chosen to be zero from the very beginning. The 'static Δg ' fit also yields a similar total χ^2 (124.28) and the idea behind this fit deserves a further explanation. If one studies the Q^2 -evolution of the total gluon polarization $\Delta g(Q^2)$ one observes that Δg rises for increasing values of Q^2 if one starts with an input $\Delta g(\mu^2) > \Delta g_{static}$. On the other hand Δg decreases for increasing Q^2 if $\Delta g(\mu^2) < \Delta g_{static}$ hence remaining constant for *all* values of Q^2 for $\Delta g(\mu^2) = \Delta g_{static}$ (cf. fig. 5). In LO the precise value of Δg_{static} can be easily obtained from the evolution equation for Δg by setting $d\Delta g(Q^2)/d\ln Q^2 = 0$. This yields

$$\Delta g_{static} \simeq -\frac{1}{2}\Delta\Sigma \approx \mathcal{O}(-0.15) \quad (11)$$

where $\Delta\Sigma = \sum_q(\Delta q + \Delta\bar{q})$ is the total helicity carried by quarks and antiquarks and (11) is only subject to a small correction in NLO.

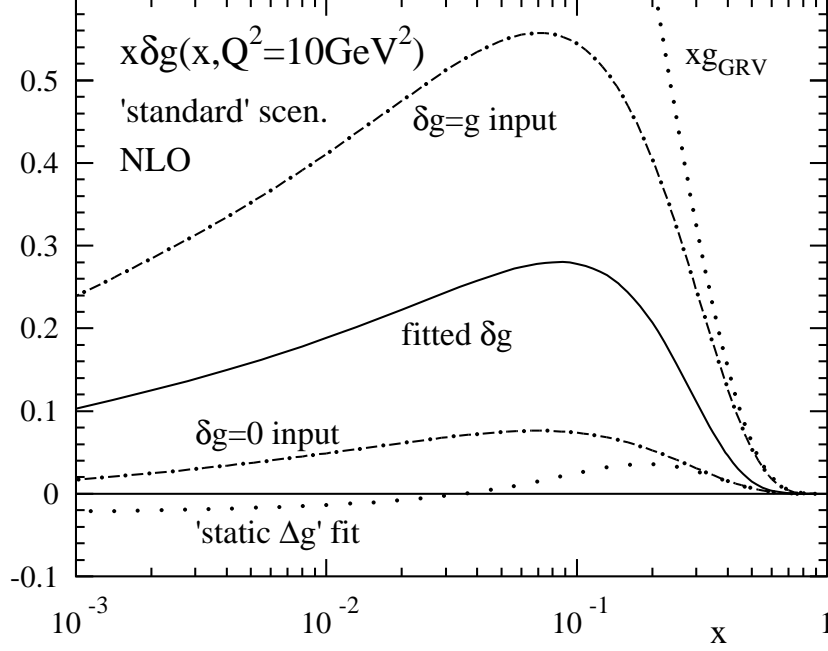


Figure 4: The experimentally allowed range of NLO polarized gluon densities at $Q^2 = 10 \text{ GeV}^2$ for the 'standard' scenario. Also shown is the unpolarized gluon distribution of ref. [15].

Fig. 2 also reveals that the valence (and to some extent also the sea) distributions are quite well determined by present data in our new fits despite of the different underlying constraints for the input distributions. On the contrary the polarized gluon density δg is still hardly constrained at all, even the rather small and 'exotic' δg resulting from the 'static Δg ' fit is not excluded.

Inevitably the large uncertainty in δg implies that also the small- x behaviour of g_1 beyond the experimentally accessible x -range is completely uncertain and not predictable as is demonstrated in fig. 3 for the proton and the neutron case in the 'standard' scenario for $Q^2 = 10 \text{ GeV}^2$. Apart from the optimal input and the already discussed 'static Δg ' fit we also present in fig. 3 the results obtained by choosing three other extreme boundary conditions for $\delta g(x, \mu^2)$. The total χ^2 values for these ' $\delta g = -g$ ', ' $\delta g = 0$ ', and ' $\delta g = g$ ' inputs are 134.68, 124.24, and 127.44, respectively. Even these inputs give still excellent fits and only the largest possible negative input in the radiative parton model (cf. eq.(5)), i.e., $\delta g(x, \mu^2) = -g(x, \mu^2)$, is disfavored by its χ^2 value. As can be seen, all these extreme inputs give indistinguishable results for $g_1^{p,n}$ in the experimentally covered x -region ($x \gtrsim 0.01$) whereas they lead to a rather large spread in the small- x region making any predictions impossible here. Note that one obtains completely similar results also in the 'valence scenario'. This uncertainty implies also a large theoretical error from the extrapolation $x \rightarrow 0$ when calculating the first moments $\Gamma_1^{p,n}$. A conservative theoretical estimate for $\Gamma_1^{p,n}$, taking into account the maximally allowed spread in $g_1^{p,n}$ by the positivity requirement (5) in the radiative parton model, i.e., ' $\delta g = -g \dots \delta g = g$ ' inputs, yields

$$\Gamma_1^p(Q^2 = 10 \text{ GeV}^2) = 0.133 \pm 0.008 \quad , \quad \Gamma_1^n(Q^2 = 10 \text{ GeV}^2) = -0.062 \pm 0.008 \quad . \quad (12)$$

Also shown in fig. 3 is the effect of not including the charm contribution to $g_1^{p,n}$ for our optimal fit results. As already mentioned in section 2, g_1^{charm} as calculated from the appropriate massive $\gamma^* g \rightarrow c\bar{c}$ subprocess [17] is negligibly small in the experimentally covered x -region and remains small even for lower values of x .

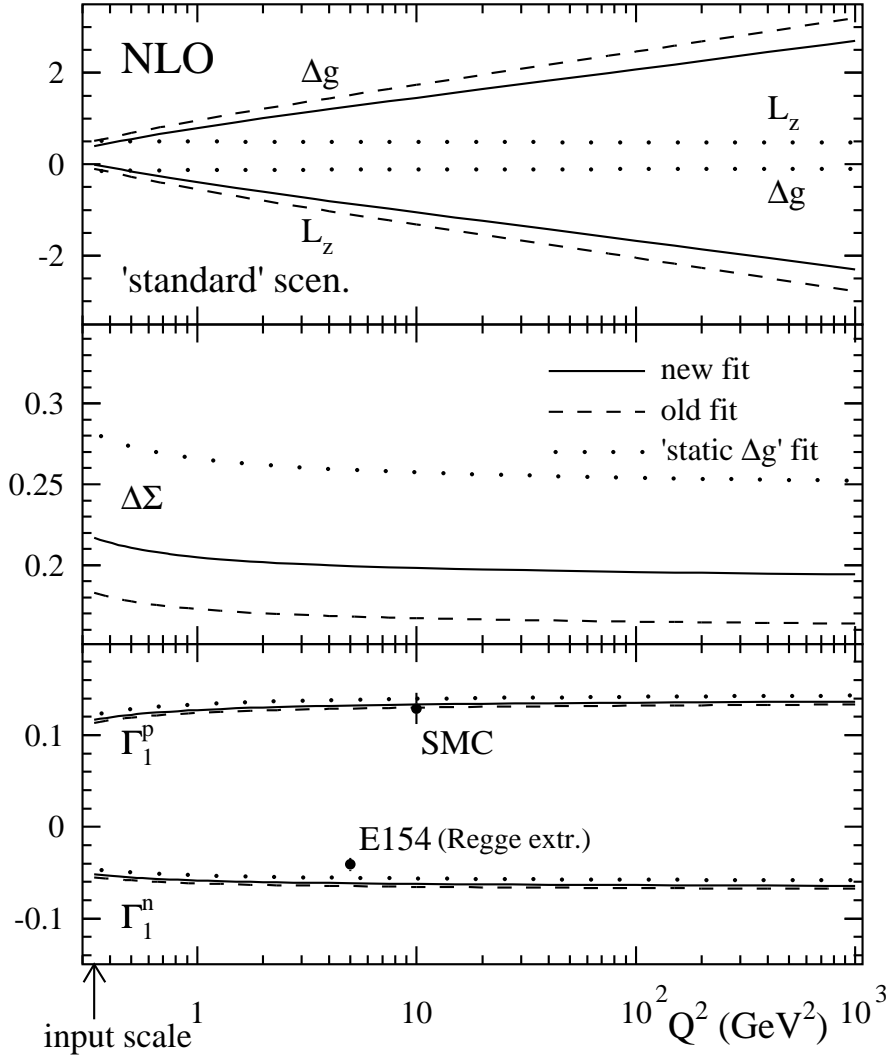


Figure 5: NLO Q^2 -evolution of the first moments Δg , $\Delta\Sigma$, and $\Gamma_1^{p,n}$ as well as of the total orbital angular momentum contribution L_z to the helicity sum rule (13) from our low input scale μ^2 up to $Q^2 = 1000 \text{ GeV}^2$ for our 'old' [8] and 'new' optimal fits as well as for the 'static Δg ' input. Also shown are some recent experimental results for Γ_1^p and Γ_1^n from SMC [5] and E154 [2], respectively.

Fig. 4 compares the different NLO gluon distributions at $Q^2 = 10 \text{ GeV}^2$ as obtained from the various inputs discussed above. It is immediately obvious that other measurements apart from DIS are required to further pin down δg . For completeness the total polarizations $\Delta g(Q^2)$ at $Q^2 = 10 \text{ GeV}^2$ for the ' $\delta g = g$ ', best fit δg , ' $\delta g = 0$ ', and 'static Δg ' inputs are 3.2, 1.45, 0.31, and -0.12, respectively. The value for the best fit gluon input is quite close to the value of 1.74 found in our previous analysis [8] and is in agreement with other fits [9, 10, 21]².

Finally, let us turn to the NLO Q^2 -evolution of the first moments $\Delta g(Q^2)$, $\Delta\Sigma(Q^2)$, and $\Gamma_1^{p,n}(Q^2)$ which is shown for the 'standard' scenario in fig. 5 for Q^2 values ranging from our low input scale μ^2 up to $Q^2 = 1000 \text{ GeV}^2$. Also shown is the Q^2 -dependence of the total orbital

²It should be noted that the possibility of having a slightly negative Δg was recently also found in [22] but without discussing the special 'static' properties of such a boundary condition.

angular momentum L_z as obtained from the helicity sum rule

$$\frac{1}{2} = \frac{1}{2}\Delta\Sigma(Q^2) + \Delta g(Q^2) + L_z(Q^2) . \quad (13)$$

It is interesting to observe that at our low input scale for our optimal fit (this hold true also for our previous results [8]) the nucleon's spin is dominantly carried just by the total helicities of quarks and gluons, i.e., $L_z(\mu^2) \approx 0$, and only during the Q^2 -evolution a large negative $L_z(Q^2)$ is being built up in order to compensate for the strong rise of $\Delta g(Q^2)$ in (13), see fig. 5.

For our 'static Δg ' fit the situation is completely different. First of all one should note that $\Delta g(Q^2)$ is indeed independent of Q^2 and quite small (cf. eq. (11)) and this in turn implies that also L_z is practically Q^2 -independent because $\Delta\Sigma(Q^2)$ is only weakly Q^2 -dependent in the $\overline{\text{MS}}$ scheme (it should be recalled that in LO $\Delta\Sigma(Q^2) = \text{const.}$). But more striking is the fact that for this boundary condition the quark and gluon contributions to the helicity sum rule (13) cancel each other (see eq. (11)) implying that for *all* values of Q^2 the proton spin is entirely of angular momentum origin. This result is quite puzzling and completely different from the intuitively expected vanishing of L_z at some low bound-state-like scale as observed for our optimal fit but cannot be excluded yet by the presently available fixed target data.

4 Summary and Outlook

We have presented an updated NLO QCD analysis of the DIS spin asymmetry $A_1^N(x, Q^2)$ data in the $\overline{\text{MS}}$ scheme in the framework of the radiative parton model. Compared to our previous results [8] we have observed a rather large change in the polarized δd_V distribution which is mainly due to new data for A_1^n , in particular from E154 [2]. In contrast to the polarized valence (and sea) quarks the gluon density $\delta g(x, Q^2)$ turns out to be still hardly constrained at all by present data. Our optimal fits, however, still favor a rather sizeable total gluon helicity, e.g., $\Delta g(Q^2 = 10 \text{ GeV}^2) \simeq 1.45$, but it was shown that even rather exotic boundary conditions for δg , with a rather small total helicity, such as the 'static Δg ' input, yield excellent descriptions of all available $A_1^N(x, Q^2)$ data.

The latter gluon input has the striking consequence that the spin of the nucleon is entirely made of orbital angular momentum for *all* values of Q^2 contrary to the intuitively expected vanishing of L_z at some low scale μ^2 as observed for our optimal fits. Finally, it was shown that the uncertainty in δg induces a rather large spread in the small- x behaviour of g_1^N making any predictions impossible. An estimate for the theoretical error in the determination of $\Gamma_1^{p,n}$ due to the $x \rightarrow 0$ extrapolation uncertainty was given.

Future fixed target DIS data, in particular from E155, as well as semi-inclusive measurements from SMC and HERMES will help to pin down the polarized quark distributions more precisely but it cannot be expected that δg can be further constrained by such measurements since the lever-arm in x and Q^2 is too limited for an indirect determination of δg from scaling-violations. A realization of the currently discussed upgrade of HERA to a polarized ep collider would be extremely helpful in this respect to gain more insight into δg as well as to pin down the small- x behaviour of $g_1^p(x, Q^2)$ more precisely.

Acknowledgements

It is a pleasure to thank M. Glück, E. Reya, and W. Vogelsang for a fruitful collaboration. I am grateful to the University of Dortmund where most of the work presented here was done. This

work was supported in part by the 'Bundesministerium für Bildung, Wissenschaft, Forschung und Technologie', Bonn.

References

- [1] P.L. Anthony et al., E142 collab., *Phys. Rev.* **D54** (1996) 6620.
- [2] K. Abe et al., E154 collab., *Phys. Rev. Lett.* **79** (1997) 26.
- [3] K. Ackerstaff, HERMES collab., *Phys. Lett.* **B404** (1997) 383.
- [4] D. Hasch, HERMES collab., invited talk in these proceedings.
- [5] B. Adeva, SMC, CERN-PPE-97-118, to appear in *Phys. Lett.* **B**.
- [6] C. Young, E155 collab., invited talk in these proceedings.
- [7] M. Glück, E. Reya, M. Stratmann, and W. Vogelsang, to appear.
- [8] M. Glück, E. Reya, M. Stratmann, and W. Vogelsang, *Phys. Rev.* **D53** (1996) 4775.
- [9] T. Gehrmann and W.J. Stirling, *Phys. Rev.* **D53** (1996) 6100.
- [10] R.D. Ball, S. Forte, and G. Ridolfi, *Phys. Lett.* **B378** (1996) 255;
G. Altarelli, R.D. Ball, S. Forte, and G. Ridolfi, *Nucl. Phys.* **B496** (1997) 337.
- [11] R. Mertig and W.L. van Neerven, *Z. Phys.* **C70** (1996) 637.
- [12] W. Vogelsang, *Phys. Rev.* **D54** (1996) 2023; *Nucl. Phys.* **B475** (1996) 47.
- [13] M. Glück, E. Reya, and W. Vogelsang, *Phys. Lett.* **B359** (1995) 201.
- [14] M. Glück, E. Reya, and A. Vogt, *Z. Phys.* **C48** (1990) 471.
- [15] M. Glück, E. Reya, and A. Vogt, *Z. Phys.* **C67** (1995) 433.
- [16] M.J. Alguard et al., SLAC-Yale collab. (E80), *Phys. Rev. Lett.* **37** (1976) 1261;
G. Baum et al., *Phys. Rev. Lett.* **45** (1980) 2000;
G. Baum et al., SLAC-Yale collab. (E130), *Phys. Rev. Lett.* **51** (1983) 1135;
J. Ashman et al., EMC, *Phys. Lett.* **B206** (1988) 364; *Nucl. Phys.* **B328** (1989) 1;
D. Adams, SMC, *Phys. Lett.* **B396** (1997) 338;
K. Abe et al., E143 collab., *Phys. Rev. Lett.* **74** (1995) 346; *Phys. Rev. Lett.* **75** (1995) 25; *Phys. Lett.* **B364** (1995) 61.
From the latter reference we have taken only those data points which correspond to the new beam energies of 9.7 and 16.2 GeV and to $Q^2 > 0.6 \text{ GeV}^2$. These points are not shown in fig. 1 but included in the fit.
- [17] A.D. Watson, *Z. Phys.* **C12** (1982) 123;
M. Glück, E. Reya, and W. Vogelsang, *Nucl. Phys.* **B351** (1991) 579.
- [18] L. Montanet et al., Particle Data Group, *Phys. Rev.* **D50** (1994) 1173;
F.E. Close and R.G. Roberts, *Phys. Lett.* **B316** (1993) 165.
- [19] H.J. Lipkin, *Phys. Lett.* **B256** (1991) 284; **B337** (1994) 157;
J. Lichtenstadt and H.J. Lipkin, *Phys. Lett.* **B353** (1995) 119.
- [20] M. Gourdin, *Nucl. Phys.* **B38** (1972) 418;
J. Ellis and R.L. Jaffe, *Phys. Rev.* **D9** (1974) 1444; **D10** (1974) 1669 (E).
- [21] K. Abe, E154 collab., *Phys. Lett.* **B405** (1997) 180.
- [22] E. Leader, A.V. Siderov, and D.B. Stamenov, hep-ph/9708335.